Supplementary Information

Dy-DOTA integrated mesoporous silica nanoparticles as promising ultrahigh field magnetic resonance imaging contrast agents

Xiao-Yu Zheng[a], Juan Pellico[a], Alexandr A. Khrapitchev[b], Nicola R. Sibson[b] and Jason J. Davis[a]*

[a.] *Department of Chemistry, University of Oxford, South Parks Road, Oxford, OX1 3QZ, UK.*

E-mail: jason.davis@chem.ox.ac.uk; Fax: +44 (0)1865 272 690; Tel: +44 (0)1865 275 914

[b.] *Cancer Research UK and Medical Research Council Oxford Institute for Radiation Oncology, Department of Oncology, University of Oxford.*

Experimental Section

Chemicals:

2,2',2''-(10-(2-((2,5-dioxopyrrolidin-1-yl)oxy)-2-oxoethyl)-1,4,7,10-tetraazacyclododecane-1,4,7-triyl)triacetic acid (DOTA-NHS-ester) was purchased from CheMatech. All other chemicals were purchased from Sigma-Aldrich and used as received. Ultrapure water (Millipore) with a resistivity of 18.2 MΩ·cm was used throughout.

Preparation of aminated MSNs by a delayed co-condensation method: Cetyl trimethylammonium bromide (CTAB, 0.64 g, 1.77 mmol) and triethanol amine (TEA, 1.03 g, 6.9 mmol) were dissolved by vigorous stirring into a mixture of ultrapure water (16.02 mL, 0.89 mol) and ethanol (1.84 mL, 0.04 mol). The solution was brought to 80 °C, and tetraethylorthosilicate (TEOS, 1.454 mL, 6.5 mmol) was added dropwise (1 mL/min) under vigorous stirring. The solution was stirred at 80 °C. Then 3-aminopropyltriethoxysilane (APTES, 2.6 µL, 10 µmol) was added after 10 min (short delay) or 60 min (long delay). The reaction was then continued at 80 °C with a total time period of 2 h. The product was collected by centrifugation (13200 rpm, 20 min) and washed with ethanol twice. To remove the

surfactant completely, the product was redispersed into an acidified ethanol solution (10 vol%) under sonication for 30 minutes and washed with ethanol twice. The product was either dried under vacuum or redispersed into ethanol depending on further use.

Preparation of aminated MSNs by a post-grafting method: Pristine MSNs were prepared via the above mentioned procedure without APTES addition. The obtained MSNs (100 mg) were dispersed into a mixture of water (5 mL) and ethanol (10 mL). Then APTES (2.6 µmol) was added and vigorous stirring was carried out at room temperature for 24 h. The aminated MSNs were washed 3 times with ethanol using centrifugation (13200 rpm, 20 min). The product was either dried under vacuum or redispersed into ethanol depending on further use.

Dy loading: Aminated MSNs (50 mg) were dispersed into anhydrous dimethylformamide (DMF, 15 mL) by sonication and stirred vigorously at room temperature for 24 h with DOTA-NHS-ester (1.25 µmol, 1 mg) and triethylamine (150 µL). The product was then washed three times with ethanol using centrifugation and redispersed into ethanol (10 mL). $DyCl_3$ (2.5 µmol) was added and vigorous stirring was carried out at room temperature for 24 h. The obtained Dy-DOTA conjugated MSNs were washed 4 times with ethanol. After drying under vacuum, the weight percentage of Dy on Dy-loaded MSNs was determined using ICP-OES to be 2.12 ± 0.66 wt% (about 17 Dy^{3+} per 100 nm^3 calculated with silica density of 2.2 g/cm^3). In a control analysis confirming the specificity of Dy localisation, pristine MSNs were directly mixed with $DyCl_3$ giving a resultant weight percentage of Dy of 0.33 ± 0.12 wt%, (confirming that 84% of Dy^{3+} ions were chelated by DOTA).

Characterization: TEM images were obtained by JEM-2100 (JEOL, Japan) operated at 200 kV. Samples for TEM were prepared by depositing and drying of a drop of an aqueous colloidal suspension of nanoparticles onto a copper grid. Average diameter was calculated by counting 50 particles. A Fourier transform infrared (FT-IR) absorption spectrometer (IRTracer-100, Shimadzu) was used to confirm the

removal of CTAB. Nitrogen adsorption-desorption analyses were performed with a Micromeritics 3Flex surface characterization analyser. DLS analysis was performed on Malvern Zetasizer Nano with a 532 nm laser as the light source. Samples for DLS were prepared by dispersing nanoparticles (*ca.* 1 mg/mL) into phosphate buffer solution (10 mM, pH = 7.4). Dy concentrations were calculated and verified using ICP-OES analysis (Optima 8000, PerkinElmer). A superconducting quantum interference device (SQUID) magnetometer was used to characterize the magnetic property of sample. For proton relaxation time measurements, nanoparticles were dispersed in ultrapure water with desired Dy concentrations, and the measurements were performed with various equipments, including Magritek Spinsolve 60 (1.4 T), Agilent DirectDrive (7.0 T), Bruker AVIIIHD 400 nanobay (9.4 T), and Bruker AVIIIHD 500 (11.7 T). A standard inversion-recovery method was used for T_1 measurement and a Carr–Purcell–Meiboom–Gill (CPMG) pulse sequence for T_2 measurements. The relaxation rate ($1/T_1$ or $1/T_2$) was plotted versus Dy concentration (mM) and relaxivities were obtained from the slope of a subsequent linear fit. Phantom images were acquired in Agilent DirectDrive (7.0 T) equipment using CPMG-base sequence (Multi-CPMG-Echos Multi-Slices) at TR = 4s and TE = 640 ms.

Figures and Tables

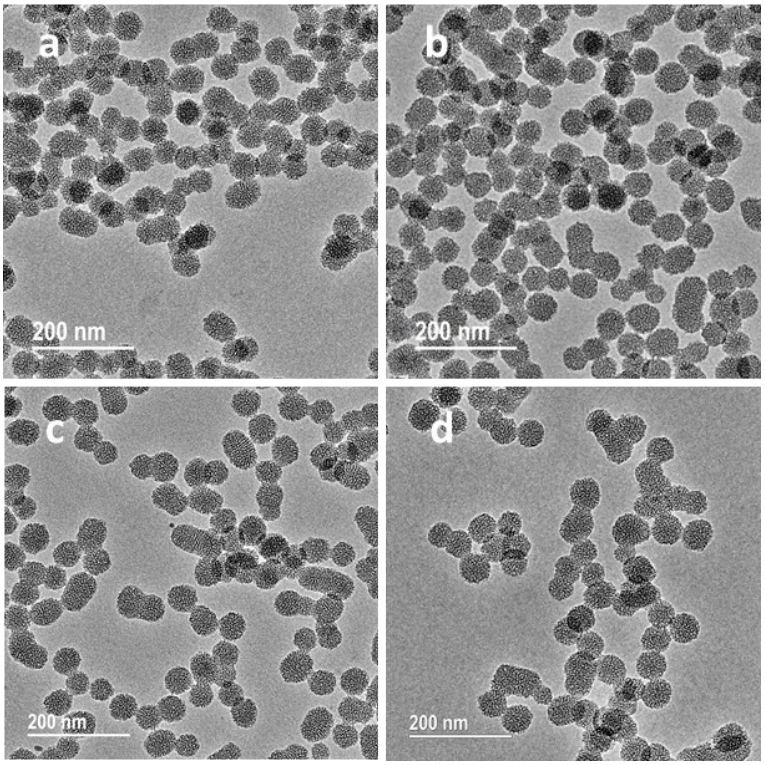

Fig. S1 TEM images of MSNs: (a) Pristine MSNs without amination, (b) Aminated MSNs prepared by "short delay" method, (c) Aminated MSNs prepared by "long delay" method, (d) Aminated MSNs prepared by "post-grafting".

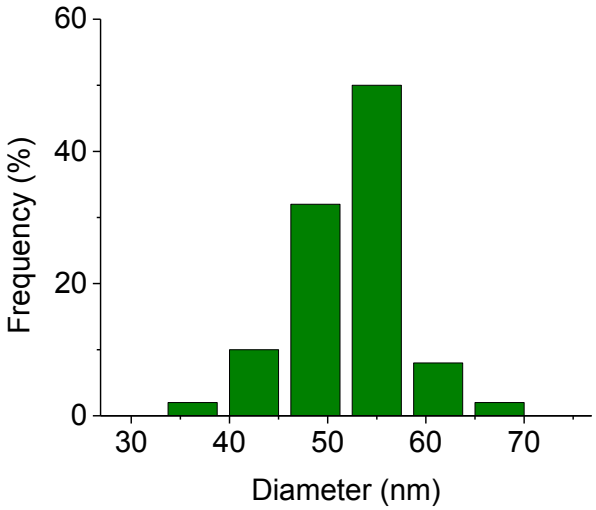

Fig. S2 The distribution of TEM size of pristine MSNs (55.7 ± 5.6 nm).

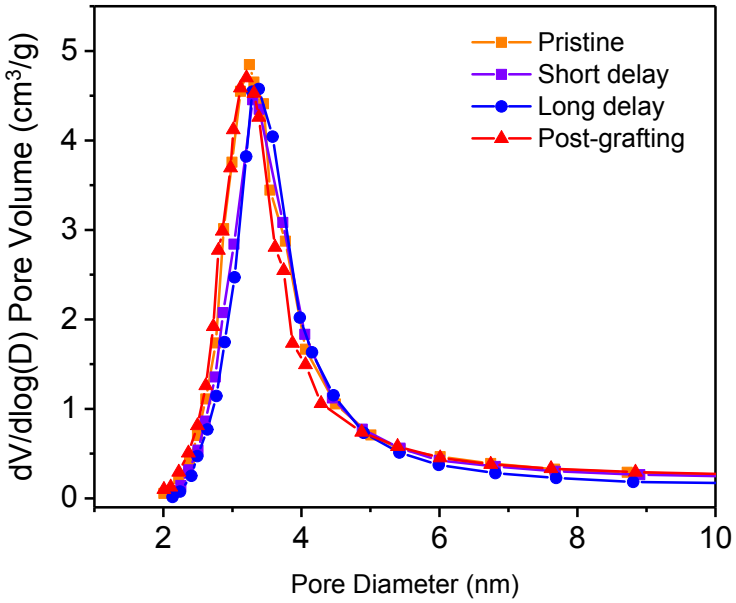

Fig. S3 Pore size distribution of MSNs with tuned amino anchor localisation. An average pore size of *ca.* 3.2 nm is calculated from adsorption using Barrrett-Joyner-Halenda (BJH) method.

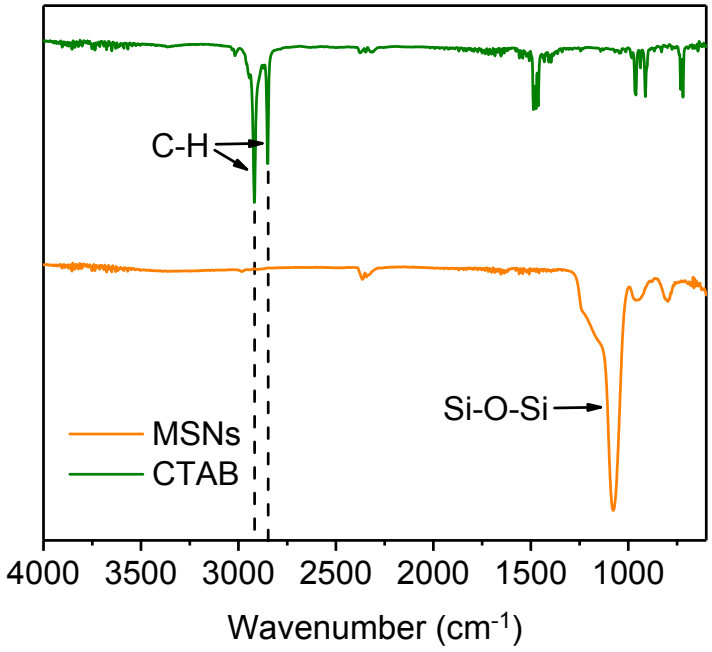

Fig. S4 FT-IR spectra of MSNs and CTAB. The characteristic peaks of CTAB at 2918 and 2848 cm^{-1} can be assigned to the stretching vibration of C–H bonds, while no characteristic peaks of CTAB can be observed in spectrum of MSNs, suggesting the complete removal of CTAB after several cycles of washing. The characteristic peak of MSNs is located at 1076 cm^{-1}, which corresponds to the Si–O–Si stretching vibration.

Table S1. Hydrodynamic size and surface zeta potential of MSNs by DLS analysis. Results are presented as mean values and standard deviations based on three measurements.

Samples	Hydrodynamic Size (nm)	S.D. (nm)	Zeta Potential (mV)	S.D. (mV)
Pristine MSNs	144.3	0.9	–32.4	1.0
Dy-MSN-S	175.3	1.2	–32.0	0.6
Dy-MSN-L	166.2	1.9	–32.8	0.5
Dy-MSN-P	160.9	1.9	-32.7	0.4

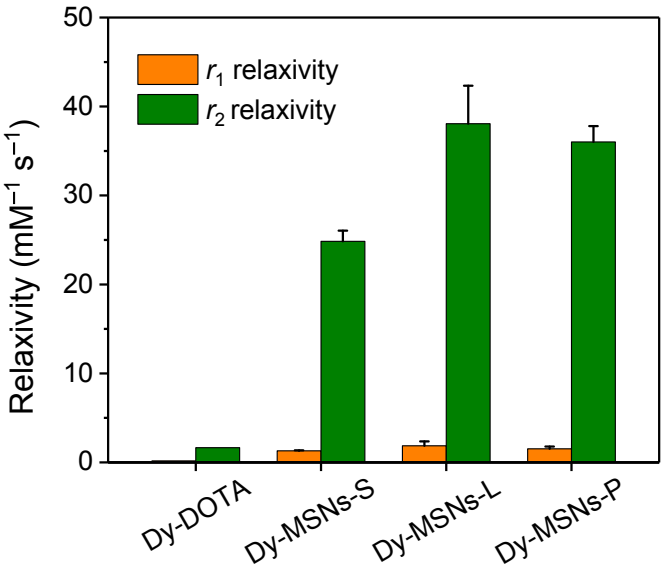

Fig. S5 Longitudinal (r_1) and transverse (r_2) relaxivity of Dy-DOTA and Dy-loaded MSNs at 7 T. Results are presented as mean value with standard deviation based on three independently prepared samples (one measurement per sample).

Table S2. Transverse relaxivity values (r_2) measured per mM of nanoparticle at different magnetic field strength.

	r_2 values (mM^{-1} s^{-1} per nanoparticle) at different magnetic fields			
Sample	**1.5 T**	**7 T**	**9.4 T**	**11.7 T**
Dy-MSNs-S	$5.2 \times 10^4 \pm 2.1 \times 10^2$	$2.5 \times 10^5 \pm 1.3 \times 10^4$	$8.8 \times 10^5 \pm 2.8 \times 10^4$	$1.2 \times 10^6 \pm 4.6 \times 10^4$
Dy-MSNs-L	$6.0 \times 10^4 \pm 2.7 \times 10^3$	$3.5 \times 10^5 \pm 2.1 \times 10^4$	$1.0 \times 10^6 \pm 1.5 \times 10^3$	$1.4 \times 10^6 \pm 2.0 \times 10^4$
Dy-MSNs-P	$5.7 \times 10^4 \pm 4.7 \times 10^3$	$3.2 \times 10^5 \pm 5.4 \times 10^3$	$9.7 \times 10^5 \pm 2.9 \times 10^4$	$1.3 \times 10^6 \pm 5.8 \times 10^3$

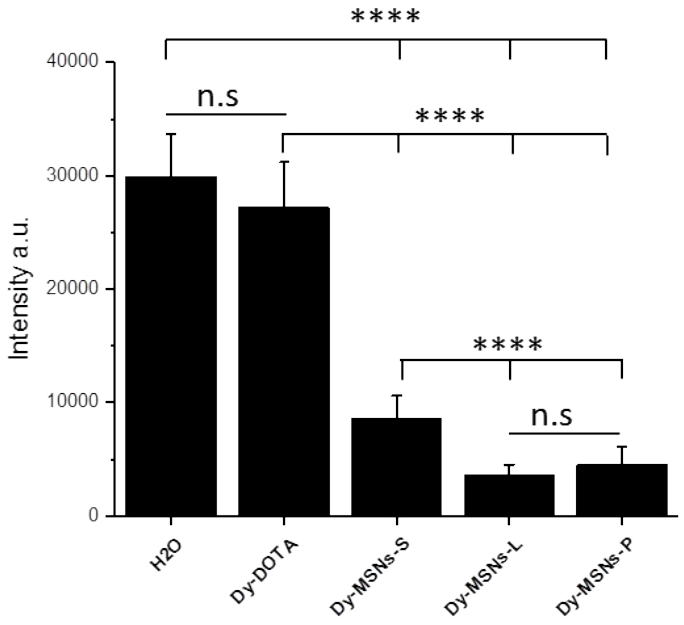

Figure S6. Region Of Interest (ROIs) intensities (a.u.) measured in phantoms acquired at 7 T for H_2O, Dy-DOTA and Dy-loaded MSNs. Statistical analysis was carried out comparing between samples by two-tailed *t*-test giving significant differences **** P<0.0001 or not significant differences n.s P>0.05.

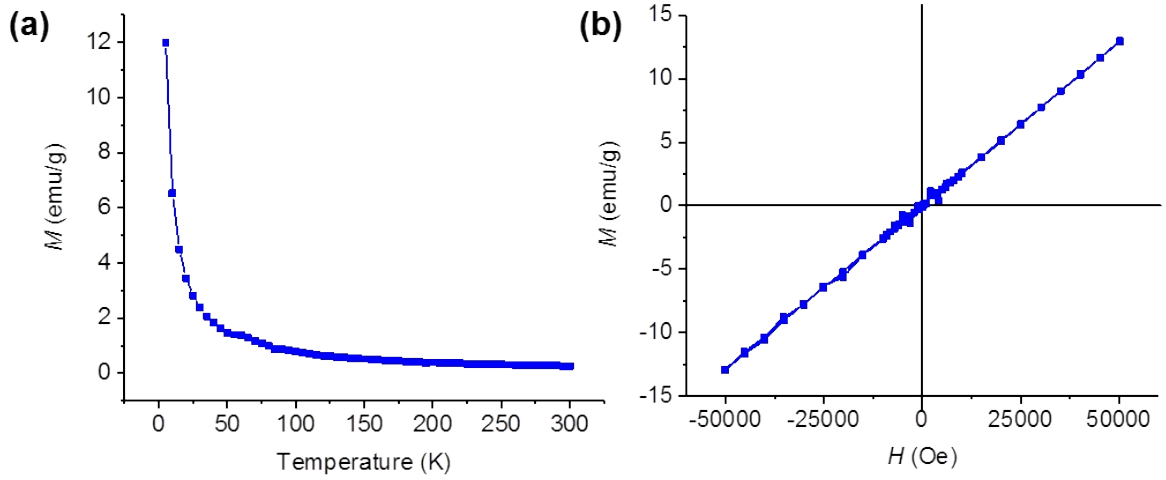

Fig. S7 (a) ZFC *M*–*T* curve at *H* = 1000 Oe and (b) *M*–*H* curve at 300 K of the powder sample of Dy-loaded MSNs. Magnetisation is normalized with the mass of Dy obtained from ICP analysis.

Theoretical simulation

Generally, the transverse relaxation rate (R_2) induced by paramagnetic species (Ln^{3+}) is the sum of inner-sphere contribution (R_2^{IS}) where water molecules are directly coordinated to Ln^{3+} and outer-sphere contribution (R_2^{OS}) where water molecules interact with ligands or freely diffuse in vicinity.[1, 2]

$$R_2 = R_2^{IS} + R_2^{OS}$$

1. Inner-sphere contribution

The inner-sphere term for transverse relaxivity (R_2^{IS}) is given by

$$R_2^{IS} = fq\frac{\frac{1}{T_{2M}^2} + \frac{1}{\tau_M T_{2M}} + \Delta\omega_M^2}{\tau_M\left(\frac{1}{\tau_M} + \frac{1}{T_{2M}}\right)^2 + \Delta\omega_M^2}.$$

R_{2M}^{IS} is the reciprocal of T_{2M}, and is the sum of three components, dipolar (R_{2D}^{IS}), Curie-dipolar ($R_{2\chi}^{IS}$), and Curie-contact (R_{2C}^{IS}) as given by:

$$R_{2M}^{IS} = R_{2D}^{IS} + R_{2\chi}^{IS} + R_{2C}^{IS},$$

$$R_{2D}^{IS} = \frac{1}{15}\left(\frac{\mu_0}{4\pi}\right)^2\gamma_I^2\mu_{eff}^2\frac{1}{r^6}\left[4\tau_{C1} + \frac{3\tau_{C1}}{1+\omega_I^2\tau_{C1}^2} + \frac{13\tau_{C2}}{1+\omega_S^2\tau_{C2}^2}\right],$$

$$R_{2\chi}^{IS} = \frac{1}{5}\left(\frac{\mu_0}{4\pi}\right)^2\gamma_I^2\mu_C^2\frac{1}{r^6}\left[4\tau_{CC} + \frac{3\tau_{CC}}{1+\omega_I^2\tau_{CC}^2}\right],$$

$$R_{2C}^{IS} = \frac{4}{3}\Delta\omega_{cont}^2\tau_M,$$

$$\tau_{Ci}^{-1} = \tau_R^{-1} + \tau_M^{-1} + \tau_{iS}^{-1} \qquad (i = 1,2),$$

$$\tau_{CC}^{-1} = \tau_R^{-1} + \tau_M^{-1},$$

$$\Delta\omega_{cont} = \frac{g_J(g_J-1)\mu_B J(J+1)B_0 A}{3k_B T\hbar}.$$

Parameters in these equations and corresponding value assignments are listed below. Note that the assumed values are all based on previous reports.[1-4]

f is the molar ratio of Ln^{3+} and water, f = 1.8×10^{-5} when [Dy] is 1 mM;

q is the number of water coordinated to Ln^{3+}, q = 1 for both Dy-DOTA and Dy-loaded MSNs;

$\Delta\omega_M$ is the ^{1}H chemical shift difference between the Ln-bound water and free water, $\Delta\omega_M/B_0$ = 1.33 ×10^5 rad·s^{-1} for both Dy-DOTA and Dy-loaded MSNs;[2]

τ_M is the residence time of coordinated water before exchanging with bulk water, τ_M = 22 ns for both Dy-DOTA and Dy-loaded MSNs;[3]

τ_{S1} and τ_{S2} are longitudinal and transverse electronic relaxation time of Dy^{3+}, respectively, and have been reported to be equal and field-independent in the range of our study, τ_{S1} = τ_{S2} = 0.33 ps;[4]

B_0 is the applied magnetic field strength;

μ_0 is the permeability of vacuum, 4π×10^{-3} H·m^{-1};

μ_{eff} is the effective magnetic moment of Ln^{3+} ($\mu_{eff} = \mu_B g_J \sqrt{J(J+1)}$);

μ_C is the Curie moment ($\mu_C = \mu_{eff}^2 B_0/(3k_B T)$);

g_J is the Landé factor of Ln, 1.333 for Dy;

μ_B is the Bohr magneton, 9.274×10^{-24} J·T^{-1};

J is the quantum number of the total spin of Ln, J = 7.5 for Dy;

γ_I is the gyromagnetic ratio of ^{1}H nucleus, 267.513×10^6 rad·s^{-1}·T^{-1};

r is the distance between Ln^{3+} and the Ln-bound water protons, we assume r = 0.3 nm for both Dy-DOTA and Dy-loaded MSNs;[4]

ω_I is the proton angular precession frequency, $\omega_I = \gamma_I B_0$;

ω_S is the electron angular precession frequency, $\omega_S = 658\omega_I$;

$\frac{A}{\hbar}$ is the hyperfine coupling constant, we assume 4.6×10^5 rad·s^{-1} for Dy;[4]

a is the hydrodynamic radius;

τ_R is the rotational correlation time ($\tau_R = 4\pi a^3 \eta / 3k_B T$);

η is the viscosity of water, 0.8949×10^{-3} Pa·s at 298 K;

k_B is the Boltzmann constant, 1.380658×10^{-23} J·K^{-1};

T is the absolute temperature, 298 K in our study.

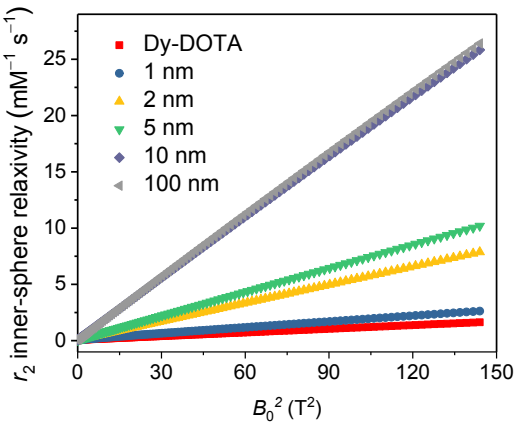

Fig. S8 Simulation curves of inner-sphere contribution to r_2 relaxivity vs. the square of external magnetic field strength at various hydrodynamic radii: 0.3 (for Dy-DOTA), 1, 2, 5, 10, and 100 nm. Other parameters are: q = 1, τ_M = 0.1 μs, r = 0.3 nm, τ_S = 0.33 ps. It is clear that the increasing inner-sphere contribution to r_2 depends on the hydrodynamic radius.

2. Outer-sphere contribution

The outer-sphere term for transverse relaxivity consists of two components, dipolar term (R_{2D}^{OS}) and Curie term (R_{2C}^{OS}).

$$R_{2D}^{OS} = \frac{32\pi}{135000}\left(\frac{\mu_0}{4\pi}\right)^2 \gamma_I^2 \mu_B^2 g_J^2 N_A \frac{M}{aD}\left[1.5j_D(\omega_I,\tau_D,\tau_{iS}) + 2j_D(0,\tau_D,\tau_{iS}) + 6.5j_D(\omega_S,\tau_D,\tau_{iS})\right]$$

$$R_{2C}^{OS} = \frac{32\pi}{45000}\left(\frac{\mu_0}{4\pi}\right)^2 \gamma_I^2 \mu_B^2 g_J^2 N_A \frac{M}{aD} \mu_C^2 \left[1.5j_\chi(\omega_I,\tau_D) + 2j_\chi(0,\tau_D)\right]$$

$$j_O(\omega,\tau_D,\tau_{iS}) = Re[\left(1+\frac{\Omega^{\frac{1}{2}}}{4}\right)/(1+\Omega^{\frac{1}{2}}+\frac{4\Omega}{9}+\frac{\Omega^{\frac{3}{2}}}{9})]$$

$$\Omega = (i\omega + 1/\tau_{iS})\,\tau_D$$

Parameters in these equations and corresponding value assignments are listed below.

M is the molar concentration of Ln^{3+};

j_O is the spectral density function (j_D and j_χ correspond to dipolar and Curie interactions, respectively);

N_A is the Avogadro number, 6.02×10^{23};

τ_D is the translational correlation time ($\tau_D = a^2/D$);

D is the relative diffusion coefficient, 2.62×10^{-9} $m^2\cdot s^{-1}$ at 298 K.

2.1 Dipolar Outer-Sphere Term

The dipolar term can also be expressed as $R_{2D}^{OS} = K_D\varphi(B_0)/a$,

where K_D is a constant, $K_D = \frac{32\pi}{135000}(\frac{\mu_0}{4\pi})^2\gamma_I^2\mu_B^2 g_J^2 N_A\frac{M}{D}$,

and $\varphi(B_0) = 1.5j_D(\omega_I,\tau_D,\tau_{iS}) + 2j_D(0,\tau_D,\tau_{iS}) + 6.5j_D(\omega_S,\tau_D,\tau_{iS})$.

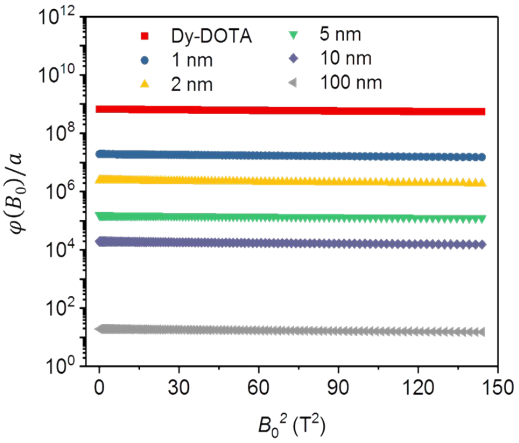

Fig. S9 Simulation curves of $\varphi(B_0)/a$ for dipolar component vs. the square of external magnetic field strength at various hydrodynamic radii: 0.3 (for Dy-DOTA), 1, 2, 5, 10, and 100 nm. Considering the dramatic change of observed r_2 relaxivity (as shown in Fig. 3) with magnetic field strength, it is

reasonable to conclude that the dipolar component does not make significant contribution to either Dy-DOTA or Dy-loaded MSNs under ultrahigh magnetic field.

2.2 Curie Outer-Sphere Term

Similarly, the Curie term can be expressed as $R_{2C}^{OS} = K_C \mu_{eff}^4 B_0^2 \theta(B_0)/a$, ,

where K_C is a constant, $K_C = \frac{32\pi}{45000}(\frac{\mu_0}{4\pi})^2 \gamma_I^2 \mu_B^2 g_J^2 N_A \frac{M}{D}(\frac{1}{3k_B T})^2$,

and $\theta(B_0) = 1.5 j_\chi(\omega_I, \tau_D) + 2 j_\chi(0, \tau_D)$.

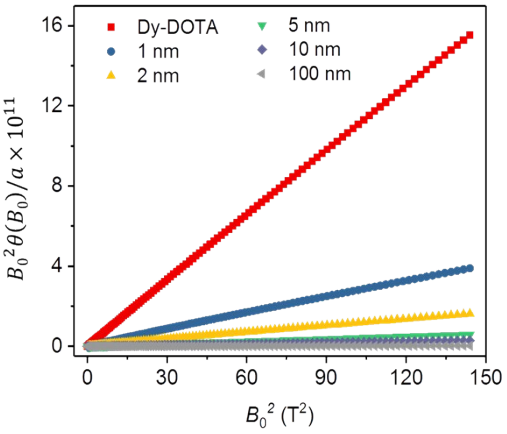

Fig. S10 Simulation curves of $B_0^2\theta(B_0)/a$ for Curie component vs. the square of external magnetic field strength. The hydrodynamic radius (a) is set to be 0.3 nm (for Dy-DOTA), and 1, 2, 5, 10, 100 nm. It can be found that with K_C and μ_{eff} fixed, the Curie contribution (R_{2C}^{OS}) actually decreases with increasing hydrodynamic radius, since the total magnetic moment is fixed in the simulation and, thus, a larger particle requires a dilution of Dy.

References

1. P. Caravan, J. J. Ellison, T. J. McMurry and R. B. Lauffer, *Chem. Rev.*, 1999, **99**, 2293.

2. M. Norek and J. A. Peters, *Prog. Nucl. Magn. Reson. Spectrosc.*, 2011, **59**, 64.

3. T. C. Soesbe, S. J. Ratnakar, M. Milne, S. Zhang, Q. N. Do, Z. Kovacs and A. D. Sherry, *Magn. Reson. Med.*, 2014, **71**, 1179.

4. L. Vander Elst, A. Roch, P. Gillis, S. Laurent, F. Botteman, J. W. M. Bulte and R. N. Muller, *Magn. Reson. Med.*, 2002, **47**, 1121.